# Chitosan/Graphene/$TiO_2$ Composites: Preparation and Its Application for Removal of Cr(VI)

Hao Zhao, Hanqiang Yu, Fengxian Qiu [a,*] and Xin Li

School of Chemistry and Chemical Engineering, Jiangsu University, Zhenjiang, 212013, China

[a]fxqiuchem@163.com

**Keywords:** Adsorption; graphene; $TiO_2$; chitosan; composites; Cr(VI).

**Abstract.** In this work, chitosan/graphene/$TiO_2$ (CS/GR/$TiO_2$) composites for the removal of Cr(VI) was prepared and characterized by FT-IR, XRD, Raman spectroscopy, TEM, SEM and $N_2$ adsorption-desorption measurements. The composites could retain large specific surface area of graphene, the mesoporous structure of $TiO_2$ and the original function of chitosan. The optimum adsorption conditions for CS/GR/$TiO_2$ composites were investigated. Kinetic data was well fitted by pseudo second-order model. Thermodynamic study indicated that the adsorption process is spontaneous and exothermic. The obtained results indicated that the prepared CS/GR/$TiO_2$ composites has potential application for the wastewater treatment containing Cr(VI).

## Introduction

Heavy metals are major pollutants of some ground and surface waters, especially in industrial waste waters. Chromium (Cr) in aquatic environments mainly come from some industrial processes such as electroplating, leather tanning and manufacturing of dyes [1]. It causes many human health problems and pollutes the environment. In recent decades, a lot of measures have been carried out for the removal of Cr(VI) ions from the environment. Among the various methods, adsorption is regarded as an efficient, versatile and cost-effective method for the Cr(VI) ions removal [2].

In this work, chitosan/graphene/$TiO_2$ (CS/GR/$TiO_2$) composites for the removal of Cr(VI) were prepared. The adsorption behavior, adsorption isotherm and kinetic model were investigated.

## Preparation of CS/GR/TiO2 composites

GO suspension was prepared [3] and was added to anhydrous ethanol (100 mL) with ultrasound for 4 h. The mixture of tetra-n-butyl titanate and HCl was stirred in the GO suspension for 0.5 h. $H_2O$ was dropped into the reaction slowly and get sol. Then, the sol was poured into hydrothermal reactor at the temperature of 180 $^oC$ for 10 h. The graphene/$TiO_2$ (GR/$TiO_2$) was washed by absolute ethyl alcohol and obtained after drying and grinding. chitosan was added to acetic and solution with ultrasound for 2 h. Next, GR/$TiO_2$ was added at 50 $^oC$ for 1.5h. The suspension was poured into hydrothermal reactor at 160 $^oC$ for 8 h. Then the solution was separated by centrifuge and washed with anhydrous ethanol and $H_2O$, respectively, until the pH of the filtrate was 7. Finally, the product chitosan/graphene /$TiO_2$ (CS/GR/$TiO_2$) composite could be obtained.

## Results and discussion

**FT-IR analysis:** FT-IR spectrum CS/GR/$TiO_2$ was recorded between 4000 and 400 $cm^{-1}$. The peaks at 1072, 1394, 1644 $cm^{-1}$ correspond to C–O–C of chitosan, C–OH stretching and C–C stretching mode of the $sp^2$ carbon skeletal network, respectively. The chitosan exhibits distinct amide I and amide II bands at 1644 and 1586 $cm^{-1}$, respectively. Moreover, the broad peaks in the region of 3000–3500 $cm^{-1}$ are related to O–H stretching and N–H stretching from chitosan. The characteristic band of the glucopyranose rings at 1162 $cm^{-1}$ also appears, which indicates that GO has been successfully deoxidized for GR and the chitosan exists on GR.

**XRD analysis:** From Fig. 1, the diffraction peaks attributed to anatase are observed in all samples. Compared with the pure $TiO_2$, the diffraction peaks in GR/$TiO_2$ and CS/GR/$TiO_2$ become wider, indicating that $TiO_2$ and chitosan could suppress the crystal growth. The typical diffraction peaks at

 

$2\theta$= 25.3°, 37.8°, 48.0°, 55.1° are ascribed to the planes of anatase form of $TiO_2$. However, no typical diffraction peaks belonging to the separate GR are observed in the composites. The fact is that the main characteristic peak of GR at 24.5° might be shielded by the main peak of anatase $TiO_2$ at 25.4°. CS/GR/$TiO_2$ composites exhibit a broad peak at $2\theta$= 20.3° due to the amorphous state of the chitosan.

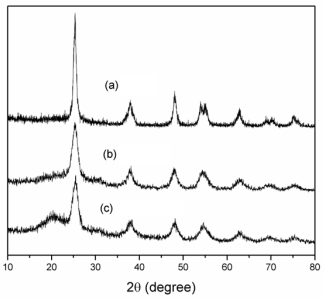


Fig.1. XRD patterns of $TiO_2$ (a), GR/$TiO_2$ (b) and CS/GR/$TiO_2$ (c)

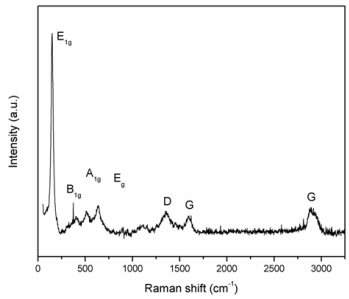


Fig. 2. Raman spectrum of CS/GR/$TiO_2$

**Raman analysis:** From Fig. 2, a very strong Raman band can be observed at 149 $cm^{-1}$ which is attributed to the main $E_{1g}$ anatase vibration mode. In addition, two bands at 1353 (D) and 1590 $cm^{-1}$ (G) which represent the graphitized structures are observed, confirming the presence of graphene. Three intense vibration peaks at 637 ($E_g$), 509($A_{1g}$) and 391($B_{1g}$) $cm^{-1}$ are also observed, indicating that the anatase $TiO_2$ crystallites are the major species. Moreover, the peak at 2888 $cm^{-1}$ (G) shows the presence of chitosan. The result further reveals the successful preparation of CS/GR/$TiO_2$.

**BET analysis:** The $N_2$ adsorption-desorption isotherms results indicate that sample has unique mesoporous structures which suggests CS/GR/$TiO_2$ is mesoporous. In addition, the isothermal type of CS/GR/$TiO_2$ is a type II adsorption–desorption, indicating adsorption is in mesopores and surfaces of the nanocomposites. From Barret-Joyner-Halenda (BJH) desorption, the BET surface area, total pore volume and average pore diameter are 40.016 $m^2/g$, 0.061$cm^3/g$ and 3.844 nm, respectively.

**TEM analysis:** From Fig. 3(a), graphene is two-dimensional layer structure. $TiO_2$ loads on the thin carbon layer evenly. From Fig. 3(b), two kinds of particles are distributed on the GR, which are $TiO_2$ and chitosan respectively. Moreover, $TiO_2$ is nanoscale spherical particles and the particle size of chitosan is larger than $TiO_2$.

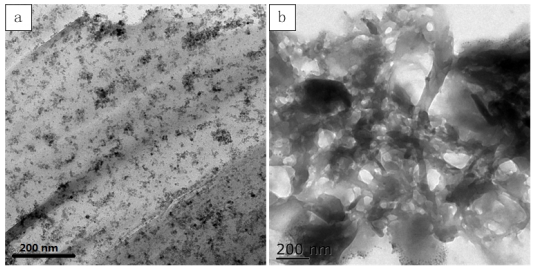


Fig. 3. TEM images of GR/$TiO_2$ (a) and CS/GR/$TiO_2$ (b)

**SEM analysis:** As can be seen from Fig. 4(a), the GR presents the sheet-like structure with the smooth surface, large thickness, and wrinkled edge with thin layer structure.

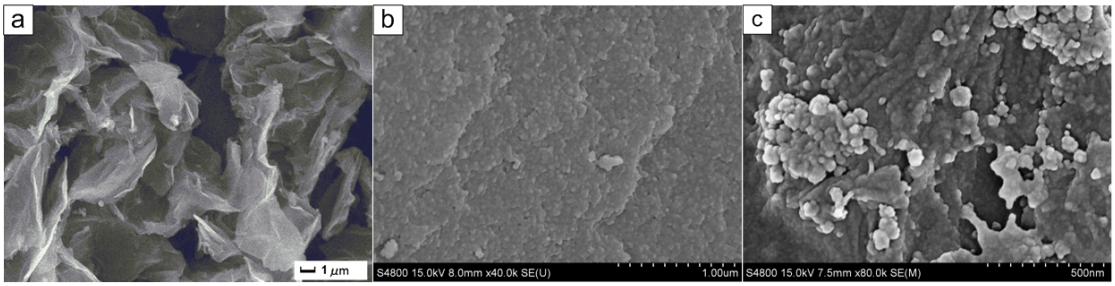


Fig. 4. SEM images of GR (a), GR/$TiO_2$ (b) and CS/GR/$TiO_2$ (c)

In Fig. 4 (b and c), the $TiO_2$ and chitosan spheres are uniformly and firmly grafted on the wrinkled GR layers with a high density. Obviously, the pleats structure of the GR may hinder the $TiO_2$–chitosan spheres from agglomeration and also make their good distribution on the GR. Moreover, the $TiO_2$–chitosan also serves as a stabilizer to avoid the aggregation of GR.

**Cr(VI) adsorption experiments:** As can be seen from Fig. 5(a), the highest adsorption efficiency is obviously obtained at the mass ratio 6:4. As shown in Fig. 5(b), the adsorption efficiency increases with the increasing of the dosage of adsorbent. However, when it is up to 20 mg/mL, adsorption efficiency changes little. So, 20 mg/mL was chosen to be the optimum dosage. From Fig. 5(c), the adsorption efficiency decreases with the increasing of temperature. The absorption procedure is exothermic reaction. So, 20 $^{o}$C was chosen in this work. As shown in Fig. 5(d), the adsorption efficiency of Cr(VI) solution increases with the absorption time increasing. When the time is more than 3 h, the adsorption efficiency changes little. Hence, 3h was selected as the optimum contact time.

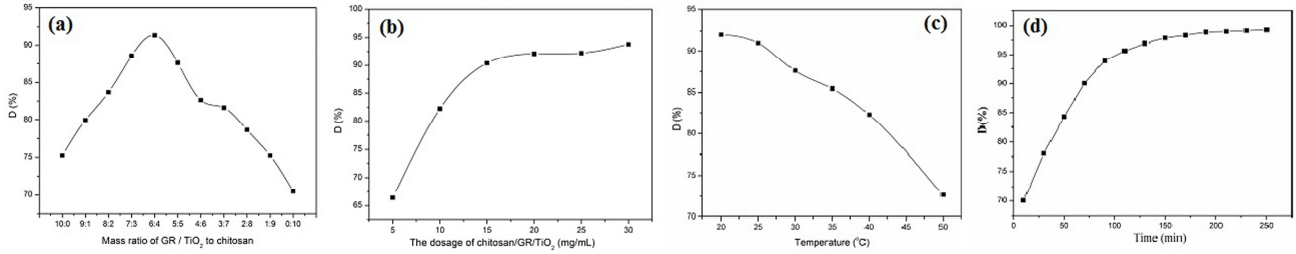


Fig. 5. Effects of mass ratio of GR /$TiO_2$(a), dosage of CS/GR/$TiO_2$(b), temperature(c) and time(d) on the adsorption efficiencies of Cr(VI) solution

**Adsorption kinetics:** The quantities of adsorbed Cr(VI) on CS/GR/$TiO_2$ material (mg/g) at different times were calculated by Eq. (1):

$$Q = \frac{V(C_0 - C)}{m} \qquad (1)$$

where Q is the amount of adsorbed Cr(VI) (mg/g), m is mass of CS/GR/$TiO_2$ and V is the volume of Cr(VI) solution (L). $C_0$ and C are the concentrations in the absence and the presence of adsorbent, respectively (mg/L).

Adsorption kinetic curve of CS/GR/$TiO_2$ towards Cr(VI) solution is shown in Fig 6(a). From Fig. 6(a), the amount of adsorbed Cr(VI) increases gradually with the time increasing. The absorption efficiency is very high during the first 3h of the process. However, the adsorption efficiency was nearly unchanged after 3h. The reason is that the adsorption of Cr(VI) has reached saturation until 3h.

The second-order kinetic model is expressed as following Eq. (2):

$$\frac{t}{Q_t} = \frac{1}{kQ_e^2} + \frac{t}{Q_e} \qquad (2)$$

where $Q_e$ and $Q_t$ are the absorption quantity at equilibrium and time of t. k is the apparent rate constant. t as abscissa and $t/Q_t$ as ordinate, linear fitting is made. The $Q_e$, K, $Q_{cal}$ and $R^2$ are 5.138 mg/g, 0.034 g $mg^{-1}min^{-1}$, 5.169 mg/g and 0.9997, respectively. The experimental data ($R^2$ = 0.9997) of adsorption of Cr(VI) is fitted to the pseudo-second-order model. The result shows that the adsorption process is dominated by pseudo-second-order adsorption mechanism.

**Adsorption isotherm:** Langmuir and Freundlich isotherms have been selected for the study. The linearized Langmuir isotherm equation is represented by:

$$\frac{1}{Q_e} = \frac{1}{Q_m} + \frac{1}{bQ_mC_e} \qquad (3)$$

where $Q_e$ is the equilibrium adsorption capacity (mg/g), $Q_m$ is the maximum adsorption capacity (mg/g), $C_e$ is the concentration of Cr(VI) in solution at equilibrium (mg/L) and b is the Langmuir affinity constant (L/mg). The data are listed in Table 1.

Table 1. Adsorption isotherms parameters for Cr(VI) adsorption onto CS/GR/$TiO_2$ composite

| Langmuir equation | | | Freundlich equation | | |
|---|---|---|---|---|---|
| $Q_m$ (mg/g) | B (L/mg) | $R^2$ | $K_f$ (mg/g) | n | $R^2$ |
| 55.43 | 0.479 | 0.9524 | 14.377 | 4.006 | 0.9927 |

The Freundlich isotherm equation is commonly expressed as follows:

$$\log Q_e = \frac{1}{n} \log C_e + \log K_f \qquad (4)$$

where 1/n, $K_f$ are empirical constant, $\log Q_e$ as the ordinate and $\log C_e$ as the abscissa drawing, linear fitting is made. If $1/n > 1$, the adsorption is harder; Otherwise, the adsorption is easier. From Table 1, the result ($1/n = 0.250$, $K_f = 14.377$mg/L) of Freundlich isotherm for Cr(VI) adsorption can be got, and the correlation coefficient is 0.9927. Compare the results above, the process of Cr(VI) adsorption confirms to Freundlich isothermal adsorption equation.

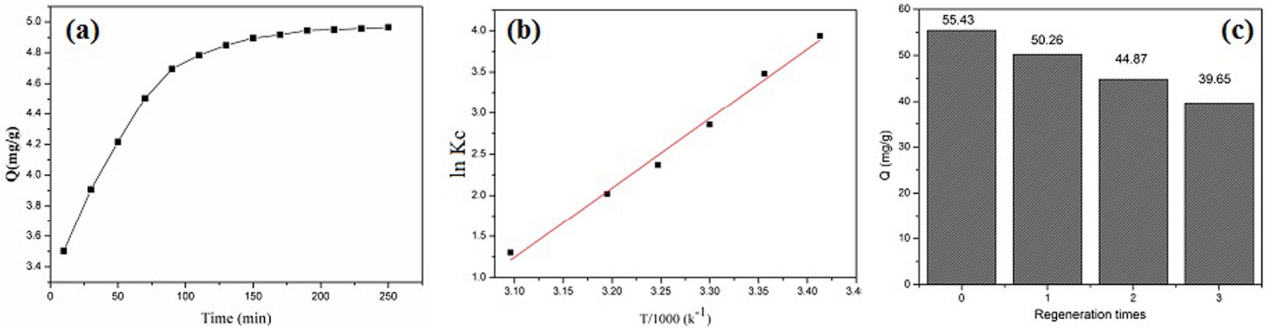


Fig. 6. Adsorption kinetic curves of CS/GR/$TiO_2$ towards Cr(VI) solution (a), van't Hoff plots for Cr(VI) adsorption(b) and effect of recycle times of CS/GR/$TiO_2$ on the adsorption efficiency of Cr(VI) solution (c)

**Thermodynamic study:** 1000/T as the abscissa, $\ln K_c$ as ordinate plot, linear fitting result is shown in Fig. 6(b). The calculated thermodynamic parameters are listed in Table 2. Negative values of $\Delta G^o$ establish the feasibility of adsorption process. Further, the increase in the values of $\Delta G^o$ with the increase of the temperature indicates that a higher temperature is not conducive to the adsorption reaction. The exothermic nature was confirmed from the negative values of enthalpy change ($\Delta H^o$), while good affinity of Cr(VI) towards the adsorbent materials is revealed by the positive value of $\Delta S^o$.

Table 2. Thermodynamic parameters for the adsorption of Cr(VI)

| T(K) | $\Delta G^0$ (KJ/mol) | $\Delta H^0$(KJ/mol) | $\Delta S^0$(J/ (mol·K)) |
|---|---|---|---|
| 293 | -9.461 | -70.21 | 207.33 |
| 298 | -8.426 | | |
| 303 | -7.389 | | |
| 308 | -6.352 | | |
| 313 | -5.315 | | |

**Desorption studies:** Fig. 6(c) presents the adsorption capacity for Cr(VI) changes from 55.43 to 39.65 (mg/g) when the process was repeated three times. After three times of desorption–adsorption, the CS/GR/$TiO_2$ composites still have high adsorption capacity. The results above indicate that CS/GR/$TiO_2$ materials are stable for Cr(VI) and have the ability of cycle.

## Conclusions

CS/GR/$TiO_2$ materials was used to remove Cr(VI) from aqueous solutions. The optimum adsorption conditions were: a dosage of CS/GR/$TiO_2$ of 20 mg/mL, a temperature of 20 $^oC$ and a time of 3h. The CS/GR/$TiO_2$ had the highest adsorption efficiency (99.5%). Kinetic studies showed that the pseudo-second order kinetics was closely followed by the adsorption reaction. Thermodynamic parameters indicated that the adsorption process is spontaneous and exothermic. The prepared material has potential application for the wastewater treatment containing Cr(VI).

## References

[1] T.S. Anirudhan, S. Jalajamony, P.S. Suchithra, Improved performance of a cellulose-based anion exchanger with tertiary amine functionality for the adsorption of chromium(VI) from aqueous solutions, Colloid. Surf. A, 335 (2009)107-113

[2] H. Deveci, Y. Kar, Adsorption of hexavalent chromium from aqueous solutions by bio-chars obtained during biomass pyrolysis, J. Ind. Eng. Chem. 19 (2013) 190-196

[3] W.S. Hummers, R.E. Offeman, Preparation of graphitic oxide, J. Am. Chem. Soc. 80 (1958) 1339-1339

 